Sains Malaysiana 51(8)(2022): 2507-2529
http://doi.org/10.17576/jsm-2022-5108-13

Synthesis of ISO Grade 46 and 68 Biolubricant from Palm Kernel Fatty Acids

(Sintesis Biopelincir ISO Gred 46 dan 68 daripada Asid Lemak Isirong Sawit)

MURAD BAHADI[1,2], JUMAT SALIMON[1] & DARFIZZI DERAWI[1,*]

[1]*Laboratory for Biolubricant, Biofuels and Bioenergy Research, Department of Chemical Sciences, Faculty of Sciences and Technology, Universiti Kebangsaan Malaysia, 43600 UKM Bangi, Selangor Darul Ehsan, Malaysia*
[2]*Faculty of Education, Hadhramout University, Hadhramout, Yemen*

Received: 5 September 2021/Accepted: 3 February 2022

ABSTRACT

Bio-based lubricant is crucial to be developed considering the toxicity risk, climate change, energy security, and green-environmental approach. Palm kernel fatty acids based biolubricants were synthesized by the homogeneous acid-catalyzed esterification reaction between palm kernel fatty acids with selected polyhydric alcohols; trimethylolpropane (TMP), di-trimethylolpropane (Di-TMP), and pentaerythritol (PE). The reaction optimization is done using a D-optimal design based on four parameters; the ratio of reactants, reaction time, reaction temperature, and catalyst loading. The optimum yield range between 80 and 87%, with more than 93% the selectivity of biolubricant products. The chemical structures of synthesized Palm kernel fatty acids-based biolubricants were characterized and confirmed using FTIR, NMR (^{1}H and ^{13}C) spectroscopies, and GC-FID chromatography. The FTIR spectra of palm kernel fatty acids-based biolubricants products clearly showed the peaks of C=O and C–O of the ester group at 1741-1740 cm^{-1} and 1234-1152 cm^{-1}, respectively. Furthermore, ^{1}H NMR spectra confirmed the ester group's proton chemical shift (-CH_2-O-) at 3.96-4.11 ppm. The ^{13}C NMR spectra confirmed the carbon chemical shifts of ester carbonyl (C=O) signals at 173.5-173.2 ppm. The results for lubrication properties have shown that the palm kernel fatty acids based biolubricants have low-temperature properties with pour points value in the range of -5 to -10 °C, a high flash point of 320-360 °C, a high viscosity index (VI) of 140.86-154.8, the kinematic viscosity of 41.76-87.06 cSt (40 °C), 8.73-14.77 cSt (100 °C), and thermal stability over 210 °C. All synthetic lubricants are categorized as ISO 46 (TMP triester) and ISO 68 (Di-TMP tetraester and PE tetraester).

Keywords: Biolubricant; fatty acids; palm kernel; polyhydric alcohols; polyol esters

ABSTRAK

Pelincir berasaskan bio adalah penting untuk dibangunkan dengan mengambil kira risiko ketoksikan, perubahan iklim, keselamatan tenaga dan pendekatan persekitaran hijau. Pelincir berasaskan asid lemak isirong sawit telah disintesis oleh tindak balas pengesteran bermangkin asid homogen antara asid lemak isirong sawit dengan alkohol polihidrik terpilih; trimethylolpropane (TMP), di-trimethylolpropane (Di-TMP) dan pentaerythritol (PE). Pengoptimuman tindak balas dilakukan menggunakan reka bentuk D-optimum berdasarkan empat parameter; nisbah bahan tindak balas, masa tindak balas, suhu tindak balas dan beban mangkin. Julat hasil optimum antara 80 dan 87%, dengan lebih daripada 93% selektiviti produk biopelincir. Struktur kimia biopelincir berasaskan asid lemak isirong sawit yang disintesis telah diciri dan disahkan menggunakan spektroskopi FTIR, NMR (^{1}H dan ^{13}C) dan kromatografi GC-FID. Spektrum FTIR bagi produk biopelincir berasaskan asid lemak isirong sawit jelas menunjukkan puncak C=O dan C–O kumpulan ester masing-masing pada 1741-1740 cm^{-1} dan 1234-1152 cm^{-1}. Tambahan pula, spektrum ^{1}H NMR mengesahkan anjakan kimia proton kumpulan ester (-CH2-O-) pada 3.96-4.11 ppm. Spektrum ^{13}C NMR mengesahkan anjakan kimia karbon bagi isyarat karbonil ester (C=O) pada 173.5-173.2 ppm. Keputusan untuk sifat pelinciran telah menunjukkan bahawa biopelincir berasaskan asid lemak isirong sawit mempunyai sifat suhu rendah dengan nilai titik tuang dalam julat -5 hingga -10 °C, takat kilat tinggi 320-360 °C, kelikatan yang tinggi. Indeks (VI) 140.86-154.8, kelikatan kinematik 41.76-87.06 cSt (40 °C), 8.73-14.77 cSt (100 °C) dan kestabilan terma melebihi 210 °C. Semua pelincir sintetik dikategorikan sebagai ISO 46 (TMP triester) dan ISO 68 (Di-TMP tetraester dan PE tetraester).

Kata kunci: Alkohol polihidrik; asid lemak; biopelincir; ester poliol; isirung kelapa sawit

Introduction

Dependence on fossil oils, global warming, and energy security are the main concerns of this century in the face of the growing industrial development and the rising standard of modernization of the World society (Prasad et al. 2020). Energy is a crucial component for all sectors of the modern economy and plays an elementary role in improving the quality of life (Bhan et al. 2020). In current situations, approximately 80% of world energy supplies rely rapidly on exhausting non-renewable fossil fuels (Gupta et al. 2013). A challenge with fossil fuel consumption is the emission of greenhouse gases (Bölük & Mert 2014). Energy security and reducing greenhouse gas emissions are the most critical priorities worldwide. Energy security is a concern due to uncertainties in supply and sudden increases in market prices of non-renewable fossil energy sources (Radovanović et al. 2017; Yaseen et al. 2020). Since the Industrial Revolution, lubricant production has been dominated by mineral-based lubricants. The use of mineral oil-based lubricants in the industries endangers toxicity issues and environmental pollutions (Mang & Dresel 2017; Mintova & Ng 2015). Much interest concerns lubricant components made from natural crop resources and biodegradable (Rudnick 2020). Utilizing bio-based and eco-friendly sources in lubricant production is getting more attention among chemists. An emerging body of work shows that excellent biodegradable ester lubricants could be produced from plant oil (Owuna et al. 2019). However, Salih et al. (2013a) noted that plants with hydrogen in their glycerol molecular backbone (in the β position) could produce lubricants with lower practical applications, as this feature would partially fragment the molecule and thus lower the thermal stability and oxidative stability of the lubricant. Bahadi et al. (2021), Resul et al. (2012), and Zulkifli et al. (2014), pointed out that there is currently much focus on researching and engineering plant-based lubricants with better stability at high temperatures, mainly via the modification of β-hydrogen active sites in the plant's triacylglycerol structure. The easiest solution is to replace the glycerol with particular polyhydric alcohol with no β-hydrogen atoms.

Pentaerythritol (PE), di-pentaerythritol (di-PE) (Cavalcanti et al. 2018), di-trimethylolpropane (di-TMP) (Nowicki et al. 2016), trimethylolpropane (TMP) (Wang et al. 2014), 2-ethyl-1-hexanol (Wu et al. 2020), and neopentyl glycol (NPG) (Papadaki et al. 2018) are some of the polyhydric alcohols commonly investigated in past research. The literature shows that esterification or transesterification commonly involves polyhydric alcohol and animal-derived or plant-derived fatty acids. Examples of plant oils that have been used are rapeseed oil, castor oil, sunflower oil, soybean oil, palm kernel oil, and Karanja oil. At the same time, animal oils that have been used include lard, yellow grease, and tallow (Karmakar et al. 2010). According to Bart et al. (2012), since these oils are highly monounsaturated, they can be used to develop lubricants that are very important to produce the liquid properties of the biolubricant base oil environmentally friendly and high performing. However, one drawback is that food demand will be indirectly impacted due to using these oils, as some are edible. Therefore, research focuses on preparing polyol esters based on non-edible oils with high fatty acids content (Agrawal et al. 2017). *Elaeis guineenisis* (oil palm tree) is a tropical industrial crop abundantly planted in Asia, Africa, and South America. Among the top exporters of crude palm oil (CPO), Malaysia and Indonesia, total oil production is about 53.3 million tonnes per year (Alam et al. 2015; Kushairi et al. 2020; Onoja et al. 2019). Mesocarp part of an oil palm fruit (Figure 1) can be extracted to produce crude palm oil (CPO), while its kernel shell provides crude palm kernel oil (CPKO) (Japir et al. 2017). Palm kernel oil (PKO) is a refined oil derived from CPKO, generally used for non-edible purposes, such as the formulations of soaps, cosmetics, and detergents (Dujjanutat & Kaewkannetra 2020). PKO has a high level of lauric acid (C12:0), which makes up an estimated 50% of its total fatty acids. The supplementary major fatty acids are myristic acid (C14:0), palmitic acid (C16:0), and oleic acid (C18:1), which make up 17, 9, and 17% of the palm kernel oil, respectively (Goon et al. 2019), making it possible to be chemically modified to produce non-food industrial products.

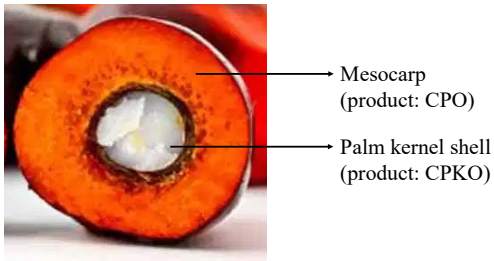

FIGURE 1. Cross-section of oil palm fruit: Mesocarp provides crude palm oil, and palm kernel shell provides crude palm kernel oil

Response surface methodology (RSM) was used in many studies to optimize the process, such as the esterification of the fatty acids and polyhydric alcohols (Aziza et al. 2014). One of the reliable common RSM modes of optimization is D-optimal design. D-optimal design is generated for multi-factor experiments with both quantitative and qualitative factors. D-optimal designs are constructed to minimize the overall generalized variance of the estimated regression coefficients. As a result, the 'optimality' of a given D-optimal design is model-dependent (Ba-Abbad et al. 2013). As a result, the 'optimality' of a given D-optimal design is model-dependent. Therefore, using D-optimal design for the optimization of esterification reactions of free fatty acids in CPKO with polyhydric alcohols will be cost-effective by reducing the amount of experiment numbers. Therefore, D-optimal design is an attractive and effective approach to optimize the synthesis of polyol ester-based biolubricant. The D-optimal design method is not limited only to evaluating the yield and selectivity of the products sought but also provides a systematic flow to obtain an optimized end result.

This work discusses the synthesis of palm kernel fatty acids based on biolubricants polyol ester through homogeneous acid-catalyzed (sulphuric acid) esterification reaction. Free fatty acids (FAs) derived from crude palm kernel oil (CPKO) served as reaction feedstock and reacted with three classes of polyhydric alcohol in acid-catalyzed esterification. Trimethylolpropane (TMP), di-trimethylolpropane (Di-TMP), and pentaerythritol (PE) were selected as the source of polyhydric alcohols, which were expected to produce a series of polyol esters-based biolubricants, namely TMP triesters, Di-TMPtetraester, and PE tetraester. Each biolubricant product was analyzed for its lubrication properties. Comparison with selected commercial lubricant products to identify the possible application of each product.

Materials and Methods

Materials

In this work, CPKO was generously supplied by Sime Darby Plantation Bhd. (647766-V), located at Selangor, Malaysia. CPKO was hydrolyzed without any pretreatment to produce CPKFAs as the reaction feedstock. Meanwhile, this study purchased all chemicals and solvents i.e., pentaerythritol (PE) 98%, Di-trimethylolpropane 97% (di-TMP), trimethylolpropane 97% (TMP), sulphuric acid 98%, sodium chloride 99.8%, ethyl acetate 99.5%, sodium bicarbonate 98%, n-hexane 99%, and anhydrous sodium sulphate 99% from Sigma Aldrich and Fisher Scientific.

Preparation of Crude Palm Kernel Fatty Acids

As per Bahadi et al. (2020), crude palm kernel oil was hydrolyzed to obtain crude palm kernel fatty acids (CPKFAs). This was manually done in batches before the synthesis of the trimethylolpropane triester. Before the process of hydrolysis, crude palm kernel oil (50 g) and 1.7 M ethanolic KOH (300 mL) was mixed in a two-necked round bottom flask at 70 °C for 2 h. Then the mixture post-hydrolysis was added with 200 mL water. Following that, 100 mL hexane was used to extract the unsaponifiable components. Approximately 60 mL of HCl 6 N was used to acidify the aqueous alcohol phase with the soap. The mixture of fatty acids (FAs) was extracted using hexane, cleansed before drying using anhydrous sodium sulfate, and then, at 45 °C, a vacuum rotary evaporator was used to evaporate it.

Polyol Ester-Based Biolubricant Production

Three biolubricant products (TMP triesters, Di-TMP tetraesters, and PE tetraesters) were synthesized in a 500 mL Dean-Stark three-necked flask. As per Rios et al. (2019), polyol esters were derived in this study via the Fischer esterification between CPKFAs (Figure 2) with three types of polyhydric alcohols (TMP, Di-TMP, and PE). A different batch of reactions was performed in selected reaction conditions. Four independent parameters (CPKFAs: alcohol ratio, reaction time, reaction temperature, and catalyst amount) were selected to optimize the reaction yield and selectivity, as part of the D-Optimal design adopted in this study. Upon reaction completion, the mixture's heating was stopped so that it could cool to room temperature, upon which 25 mL of ethyl acetate was added. A 100 mL separation funnel was prepared to which the mixture was transferred and then shaken together with 10 mL of saturated sodium bicarbonate ($NaHCO_3$). Then, the funnel separator was left until two layers formed. It could be observed that once the aqueous layer at the bottom was removed, an organic layer remained. This organic layer has washed a total of five times; thrice with a sodium bicarbonate ($NaHCO_3$) solution and then twice using 10 mL of distilled water and 10 mL of saturated sodium chloride (NaCl) to prevent the formation of an emulsion. After placing the sample in a small beaker, the remaining water was absorbed using sodium sulfate (Na_2SO_4). To further purify the sample, filtration of the hydrated Na_2SO_4 was done. A rotary evaporator at 80 °C was then used to remove ethyl acetate from the column product, producing polyol esters as a viscous liquid (Ahmed et al. 2015).

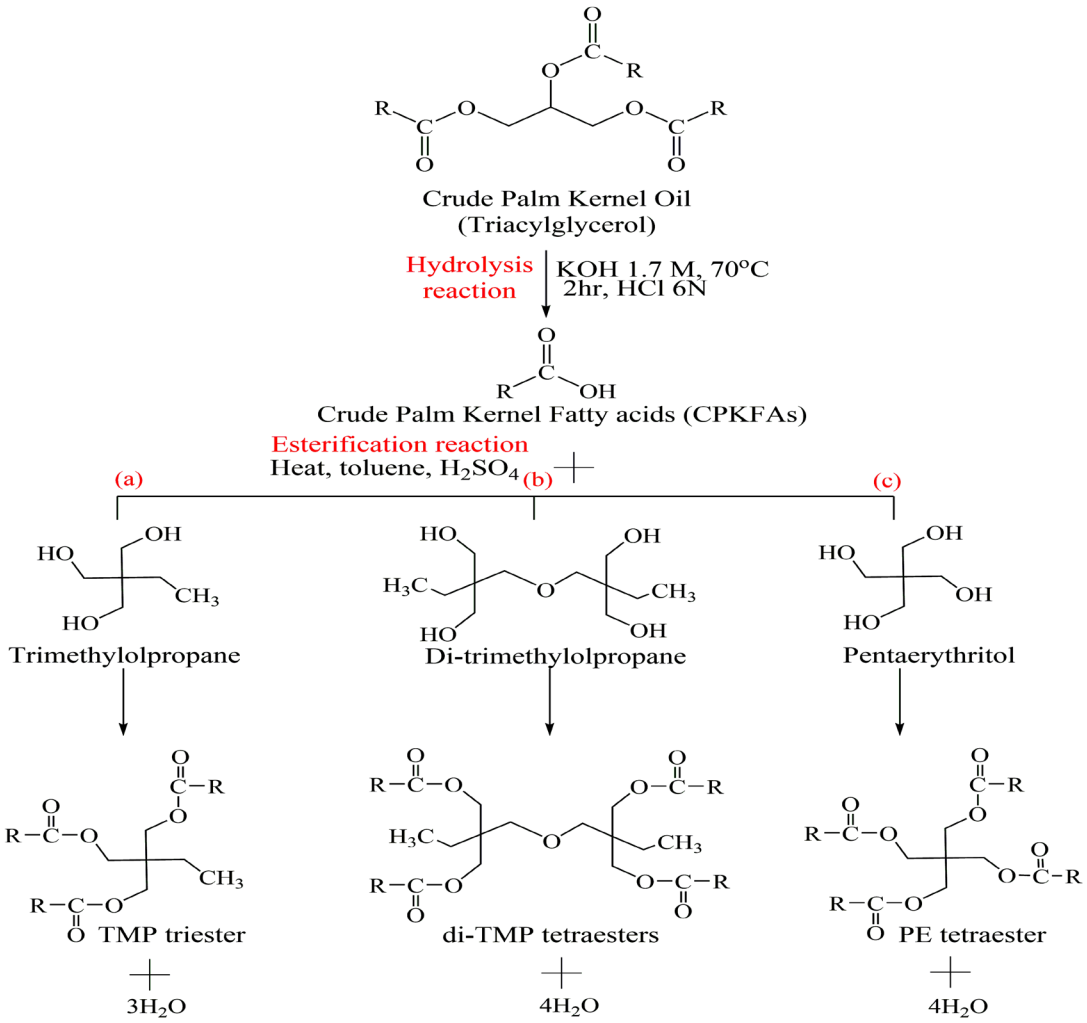

FIGURE 2. Schematic representation of the esterification reaction of CPKFAs with TMP (a), di-TMP (b), and PE (c). R = (Caprylic acid $C_{8:0}$, Capric acid $C_{10:0}$, Lauric acid $C_{12:0}$, Myristic acid $C_{14:0}$, Palmitic acid $C_{16:0}$, Stearic acid $C_{18:0}$, Oleic acid $C_{18:1}$and Linoleic acid $C_{18:2}$)

OPTIMIZATION OF SYNTHESIS PARAMETERS

This study attempted to develop polyol esters biolubricant derived from crude palm kernel fatty acids and producing trimethylolpropane triesters (TMP triester), di-trimethylolpropane tetraesters (Di-TMP tetraester), and pentaerythritol tetraester (PE tetraester). For each product, two responses were being monitored: The yield and selectivity. The yield and selectivity depended on the set of the condition of parameters; those were the ratio of CPKFAs-to-polyhydric alcohols (TMP, Di-TMP, and PE), reaction temperature, reaction time, and catalyst amount (% H_2SO_4). The varying sets of conditions were constructed via a four-factor D-optimal design. The independent variables were labeled as A for CPKFAs-to-polyhydric alcohols (TMP, di-TMP, or PE) ratio (mol:mol), B for reaction temperature (°C), C for reaction time (h), and D for the catalyst amount (% H_2SO_4). The low value (-1) and high value (+1) of A, B, C, and D can be referred from Table 1. The execution of the experiment based on the D-optimal design has generated 25 runs each for the synthesis of TMP triesters, di-TMP tetraesters, and PE tetraesters, as listed in Tables 2, 3, and 4, respectively. Experimental reaction yield and selectivity of TMP triesters, Di-TMP tetraesters, and PE tetraesters are expressed as Equations (1), (2), and (3).

$$Yield\ (\%) = \frac{\text{weight final}}{\text{weight reactants}} \times 100 \qquad (1)$$

$$Selectivity\ of\ TMP\ triester\ (\%) = \frac{\text{area tri}}{\text{area mono} + \text{area di} + \text{area tri}} \times 100 \quad (2)$$

$$Selectivity\ of\ Di-TMP\ tetraester\ or\ PE\ tetraester\ (\%) = \frac{\text{area tetra}}{\text{area mono} + \text{area di} + \text{area tri} + \text{area tetra}} \times 100 \quad (3)$$

TABLE 1. Parameters and levels for D-optimal design of the synthesis parameters

Parameters	Symbol	Unit	Parameters levels		
			-1	0	+1
TMP triester					
The CPKFA/TMP ratio	A	mol:mol	3	3.5	4
Reaction time	B	h	3	4.5	6
Reaction temperature	C	°C	110	130	150
Catalyst amount (H_2SO_4)	D	wt. %	1	3	5
Di-TMP tetraester					
The CPKFA/di-TMP ratio	A	mol:mol	4	4.5	5
Reaction time	B	h	3	4.5	6
Reaction temperature	C	°C	120	140	160
Catalyst amount (H_2SO_4)	D	wt. %	1	3	5
PE tetraester					
The CPKFA/di-TMP ratio	A	mol:mol	4	4.5	5
Reaction time	B	h	4	5	6
Reaction temperature	C	°C	150	160	170
Catalyst amount (H_2SO_4)	D	wt. %	1	3	5

CHEMICAL COMPOSITIONS ANALYSIS

Composition of the TMP triesters, Di-TMP tetraesters, and PE tetraesters was determined using the gas chromatographic (Aziza et al. (2014). The samples were prepared by diluting 0.01 ± 0.005 g with 1.0 mL of ethyl acetate in a 2.0 mL vial before being injected into the gas chromatography system. The mixture was swirled to dissolve the solvent and after that 0.5 mL of N, O-bis (trimethylsilyl) trifluoroacetamide (BSTFA) was added. After thorough swirling, the sample was heated in the 40 °C water bath for about 10 min. The sample was left to cool to room temperature then injected on the GC-FID. The analysis was performed using a DB-5HT (30 m × 0.25 mm × 0.01 μm). As the carrier gas for the GC system, Helium was injected at a flow rate of 1 μL of the sample. The injector and detector were adjusted at 380 and 400 °C, respectively. The oven temperature was set to 100 °C for 1 min during the first holding time. The ramping rate was elevated to 5 °C/min until 380 °C has been reached, and it was kept constant for 80 min. The peaks were identified by comparing the retention time to authentic standards.

While the fatty acids composition of polyol esters products was determined using GC instrument (Shimadzu GC-17A). The GC capillary column (BPX 70) was adjusted using the following temperature program: i) 120 °C, with a 3 °C increment per min for 57 min. The injector temperature was then set to 260 °C, while the detector temperature was 280 °C. The carrier gas was helium, with a 0.3 mL/min flow rate. The methods outlined in Bahadi et al. (2016) were used to set the GC parameters in this study. The method outlined in Japir et al. (2016) was used to carry out the base-catalyzed transesterification of CPKO

and the polyol ester products acid-catalyzed esterification of CPKFAs to prepare the fatty acid methyl ester (FAME). Following that, the retention times were compared with authentic standards to identify the peaks.

MOLECULAR CHARACTERIZATION

Nuclear Magnetic Resonance (NMR) spectroscopy was used to identify the chemical structure of TMP triesters, di-TMP tetraester, and PE tetraester, adopting the methods of Aigbodion and Bakare (2005) and Awang et al. (2007). NMR spectra identify the chemical structure of molecules from the absorbed electromagnetic radiation in the radio frequency (Pavia et al. 2015). Next, ^{13}C and ^{1}H NMR analyses were performed with a Joel FCP model at 400 MHz and the solvent $CDCl_3$. Then, ^{13}C and ^{1}H NMR spectra of the products were recorded on a Bruker 400 NMR spectrophotometer, where 10 mg of sample were dissolved in 560 µL of $CDCl_3$. The samples were inserted into a glass tube before introducing them into the NMR tube. The functional groups in TMP triesters, Di-TMP tetraester, and PE tetraester were determined using Fourier transform infrared (FTIR spectroscopy was carried out) according to Rohman et al. (2010). The FTIR spectra of samples were obtained with a Perkin Elmer Spectrum GX spectrophotometer in the range of 400-4000 cm^{-1} wavenumbers. A drop of each sample was spread into a thin layer on the NaCl cells (25 × 4 mm thickness) and was used for analysis.

LUBRICANT CHARACTERIZATION

Different physicochemical techniques were used to analyze the biodegradable polyol ester products. The oxidative stability of biodegradable polyol ester products was tested using a Pressurized Pressure Differential Scanning Calorimetry (PDSC) DSC 822e Mettler Toledo calibration model. StarE software was also used. This device is useful for evaluating the oleochemicals' oxidative stability temperature (Abdullah et al. 2016). Following that, heat flow (W/g) was plotted against temperature. The maximum signal temperatures (SMT, °C) and oxidation onset (OT, °C) were calculated from this plot. The thermal decomposition of the TMP triester, di-TMP tetraester, and PE tetraester was conducted using a NETZSCH STA 449 F3 Jupiter® TG/DTA thermal analyzer under nitrogen gas flow with a heating rate of 10 °C/min with varying the temperature from 25 to 800 °C (Algoufi et al. 2017). Usually, the properties of fluids at low temperatures can be determined from their pour point, which is the lowest temperature at which the fluid remains fluid and can still be poured (Salih et al. 2013b). This study determined the polyol ester products' pour point based on ASTM D5949 (Salimon et al. 2012; Yunus et al. 2005). According to ASTM D 56-79 was used to determine the higher liquid temperature that would ignite the vapor test specimen when a test flame was passed over it, also known as the flashpoint. The test involves pouring the sample into a test cup up to a temperature range of 0 to 500 °C. First, a test cup was prepared, to which approximately 10 mL of the test specimen was poured. The product was then heated continuously until it reached 100 °C. Then, closer to the flashpoint, the temperature was stepped up slowly and continuously at 5 °C. A spark plug was then used to pass a test flame across the cup at specified intervals (Salih et al. 2011). At 40 and 100 °C, Anton Paar equipment measured the product's viscosity. ASTM D445-97 was used to measure the kinematic viscosity, while ASTM D2270-93 was used to calculate the viscosity index. The four-ball method (PCS Instruments, London, UK) via Laser Scientific (Granger, IN, USA) outlined in ASTM D4172-94 was used to determine the product's tribological properties. While rheological properties of lubricant products were observed using a rheometer instrument equipped with cone/plate geometry (Derawi & Salimon 2013). A 0.051 mm diameter cone with a CP 25-2 spindle was used for the rheometer. The manipulation of the shear rate was done at 25 °C between 0–100 s^{-1}.

Results and Discussion

Before esterification, crude palm kernel fatty acids (CPKFAs) were acquired from the hydrolysis of crude palm kernel oil. The polyol ester biolubricant, TMP triesters, Di-TMP tetraesters, and PE tetraesters were synthesized in this study by conducting the esterification of CPKFAs with three types of polyhydric alcohols (TMP, Di-TMP, and PE) in the presence of sulphuric acid (H_2SO_4) as homogeneous catalyzed. Figure 2 shows the scheme of the esterification of CPKFAs with TMP, Di-TMP, and PE. In the esterification reaction of CPKFAs with TMP, monoester and diester compounds were produced throughout the reaction as side products, while the major product was a triester compound, CPKFAs-TMPTE. Meanwhile, the esterification of TMPs with Di-TMP has produced the monoester, diester, and triester compounds throughout the reaction as side products.

In contrast, the major product was a tetraester compound, CPKFAs-di-TMPTE. Monoester, diester, and triester compounds were produced throughout

the esterification of CPKFAs with PE as side products, while the major product is tetraester compound, CPKFAs-PETE. Response surface methodology with D-optimal design was introduced to obtain the optimum yield and selectivity of the products. Tables 1, 2, and 3 represents tabulated experimental data based on selected parameters; the CPKFAs/polyhydric alcohols ratio, reaction time, temperature, and catalyst amount. Both reaction yield and selectivity of all products (the composition of CPKFAs-TMPTE, CPKFAs-di-TMPTE, and CPKFAs-PETE) are recorded in Tables 2, 3, and 4 respectively.

TABLE 2. Optimization of process parameters in TMP triester production

Run	CPKFAs:TMP ratio (mol:mol)	Reaction time (h)	Reaction temperature (°C)	Catalyst amount (%)	Reaction yield %	Selectivity of triester %
1	3.5	6.0	130	3	88	99
2	3.0	3.0	110	1	64	90
3	3.0	4.5	110	5	68	73
4	4.0	4.5	130	3	69	86
5	3.5	4.5	130	1	84	99
6	4.0	3.0	110	3	53	76
7	3.0	3.0	150	3	73	87
8	4.0	3.0	150	5	71	69
9	3.0	4.5	130	3	76	93
10	4.0	3.0	150	5	71	70
11	4.0	3.0	150	1	73	92
12	3.5	3.0	130	3	82	96
13	3.0	6.0	150	5	83	95
14	3.0	6.0	110	3	70	82
15	4.0	3.0	150	1	72	93
16	3.0	3.0	110	1	63	89
17	4.0	6.0	150	3	74	78
18	4.0	6.0	110	1	69	73
19	4.0	6.0	110	5	82	88
20	3.50	3.0	110	5	75	77
21	4.0	6.0	110	5	84	86
22	3.0	6.0	150	5	84	96
23	3.0	3.0	130	5	86	83
24	3.5	4.5	130	4	79	91
25	3.0	6.0	150	1	87	99

TABLE 3. Optimization of process parameters in Di-TMP tetraester production

Run	CPKFAs:di-TMP ratio (mol:mol)	Reaction time (h)	Reaction temperature (°C)	Catalyst amount (%)	Reaction yield %	Selectivity of tetraester %
1	4.0	6.0	120	1	80	97
2	4.5	4.5	140	3	78	91
3	4.0	3.0	120	5	67	89.
4	5.0	6.0	120	1	79	93
5	4.0	3.0	120	1	78	94
6	5.0	3.0	160	5	65	88
7	4.5	6.0	160	1	82	95
8	4.0	4.5	160	5	73	93
9	4.0	4.5	120	1	77	96
10	5.0	3.0	160	5	62	87
11	4.0	3.0	160	1	73	88
12	4.0	6.0	140	1	88	95
13	4.5	3.0	120	1	83	95
14	4.0	6.0	160	3	77	95
15	5.0	4.5	160	1	69	90
16	5.0	3.0	140	1	74	85
17	4.0	6.0	120	5	81	82
18	5.0	6.0	120	5	80	68
19	4.0	6.0	160	3	75	94
20	4.5	4.5	140	3	77	93
21	5.0	6.0	120	1	79	92
22	5.0	3.0	120	1	77	92
23	4.0	4.5	160	5	75	92
24	5.0	6.0	160	5	77	78
25	5.0	3.0	120	5	72	75

TABLE 4. Optimization of process parameters in PE tetraester production

Run	CPKFAs: PE ratio (mol:mol)	Reaction time (h)	Reaction temperature (°C)	Catalyst amount (%)	Reaction yield %	Selectivity of tetraester %
1	5.0	5.0	170	1	64	75
2	4.5	4.5	160	3	84	95
3	4.0	5.0	160	3	81	71
4	5.0	6.0	150	1	78	87
5	5.0	4.0	150	1	67	73
6	4.0	4.0	170	1	87	93
7	5.0	5.0	150	5	80	76
8	5.0	4.0	160	5	69	60
9	4.0	4.0	150	5	86	96
10	4.0	5.0	170	5	68	74.
11	4.0	6.0	170	1	74	76
12	4.0	5.0	150	1	75	72
13	4.0	4.0	170	1	85	95
14	5.0	6.0	170	5	67	47
15	4.5	5.0	170	3	79	87
16	4.0	4.0	150	5	83	94
17	4.5	4.0	170	5	80	89
18	5.0	6.0	170	5	69	50
19	4.5	5.0	150	3	87	85
20	5.0	6.0	150	1	76	85
21	4.5	6.0	160	3	81	82
22	4.0	6.0	150	5	61	57
23	5.0	5.0	160	3	72	60
24	5.0	4.0	170	3	61	53
25	5.0	4.0	150	1	66	71

THE EFFECTS OF PARAMETERS ON THE RESPONSES

Figure 3 shows the effect of input parameters on reaction yield and selectivity of TMP triester. The perturbation plots provide useful demonstration on the relationship of CPKFAs/TMP ratio (A), reaction time (B), reaction temperature (C), and catalyst amount (D) on the reaction yield, and to compare the effects of all the factors at a particular point in the design space. From the perturbation plot, the greater main effect is depicted by a line with a steeper slope for long-range change. The plot of reaction yield of the TMP triester shows that reaction time (B), reaction temperature (C), and catalyst amount (D) have

a significant positive effect on the TMP triester as the level changed from low to high, as shown in Figure 3(a). Conversely, the reaction yield was affected negatively by CPKFAs/TMP ratio (Figure 3(a)) where TMP triester production decrease from 78 to 65% as A was increased from 3 to 4 mol. Note that the steeper slope of reaction time and reaction temperature in Figure 3(a) was for a longer time range, thus, suggesting greater main effect.

The main effect plots for TMP triester selectivity is shown in Figure 3(b). It appears that the pattern was somewhat similar with the yield response, but the slope is less steep for most of the parameters in affecting the TMP triester selectivity. The slope of the TMP triester selectivity line versus the CPKFA/TMP ratio shows a substantial decrease in the value of TMP triester selectivity when CPKFA/TMP ratio was increased from low level (3 mol) to high level (4 mol) (Figure 3(b)). The TMP triester selectivity did not significantly changed when reaction time increased from low level (3 h) to high level (6 h) (Figure 3(b)). Contrariwise, the plot in Figure 3(b) shows the positive effect of reaction temperature on TMP triester selectivity from the low level (110 °C) to the high level (135 °C). There was a significant negative effect against the selectivity from low level (1%) to high level of the amount catalyst (5%) (Figure 3(b)).

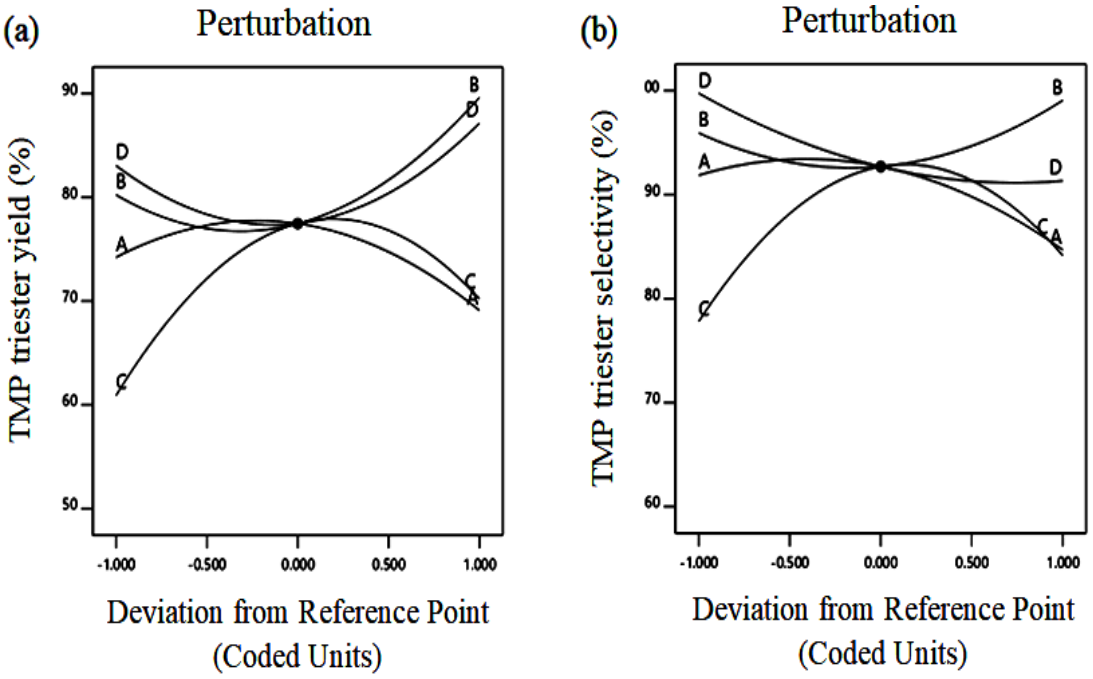

FIGURE 3. Perturbation effect plot of all the factors CPKFAs/TMP ratio (A), reaction time (B), reaction temperature (C), and Catalyst amount (D) for (a) TMP triester yield and (b) TMP triester selectivity by RSM

Figure 4 shows the correlation between the main parameters and responses of Di-TMP tetraester production. In reaction yield of Di-TMP tetraester, it can be observed from the plot that the yield of Di-TMPtetraester was highly influenced the reaction time, compared to other parameters. Figure 4(a) shows that the yield of di-TMP tetraester was affected in a significantly positive way by the reaction time from the low level (3 h) to the high level (6 h). Meanwhile, the yield of di-TMP tetraester negatively correlates against CPKFAs/di-TMP ratio, reaction temperature and catalyst amount from low to high level as shown in Figure 4(a). Therefore, the peak points of all independent parameters were 4.4 mol CPKFAs /di-TMP ratio, 6 h of reaction time, 135 ℃ reaction temperature, and 1% H_2SO_4 catalyst amount. These values are the individual optimal condition to obtain a maximum yield of Di-TMP tetraester.

For the Di-TMP tetraester selectivity, the individual effect of parameters was plotted as the response mean for each factor level connected by a line. Figure 4(b) illustrates a series of one-factor plots for each parameter. Attention was made towards the plots with a line with

a steeper slope that indicates a greater main effect in contributing a higher selectivity of di-TMP tetraester. The plots for CPKFAs/Di-TMP ratio, reaction time and catalyst amount show a negatively significant effect from low to high level as shown in Figure 4(b). However, a thoughtful finding is the plot of reaction time which shows a rather flat slope among other parameters. It can be concluded that the reaction time factor may not be significant enough to affect the Di-TMP tetraester selectivity. Conversely, the plot for the Di-TMP tetraester selectivity against reaction temperature shows a significant positive effect from low level to high level in Figure 4(b).

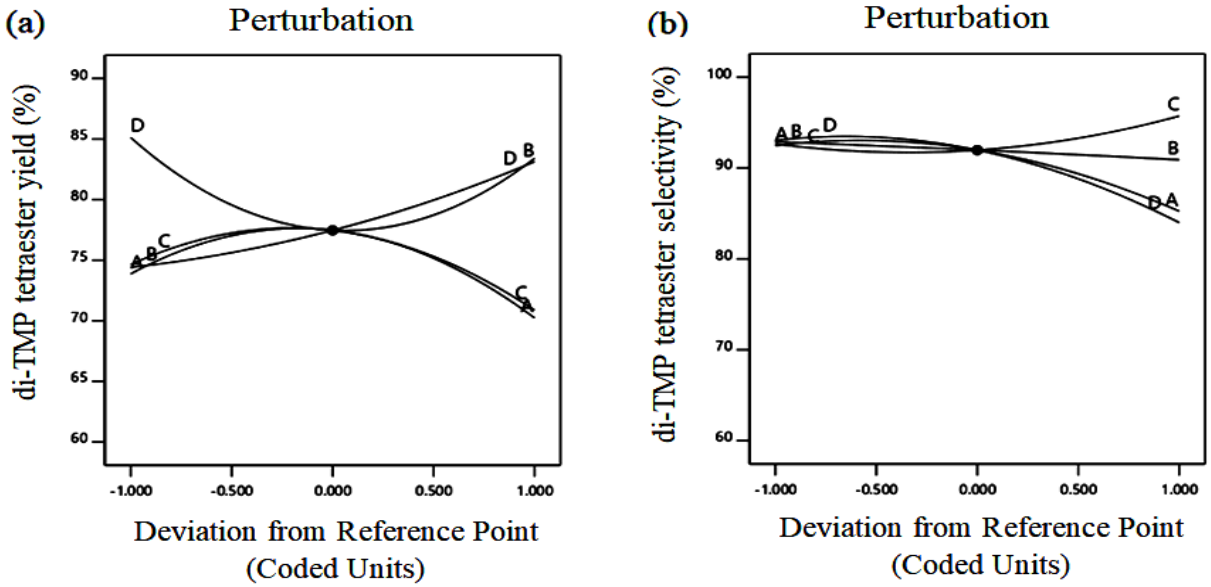

FIGURE 4. Perturbation effect plot of all the factors CPKFAs/di-TMP ratio (A), reaction time (B), reaction temperature (C), and Catalyst amount (D) for (a) Di-TMP tetraester yield and (b) di-TMP tetraester selectivity by RSM

The effect of input parameters on reaction yield and selectivity of PE tetraester as shown in Figure 5. The perturbation plots provide useful demonstration on the relationship of CPKFAs/PE ratio (A), reaction time (B), reaction temperature (C), and catalyst amount (D) on the reaction yield, and to compare the effects of all the factors at a particular point in the design space. From the perturbation plot, the greater main effect is depicted by a line with a steeper slope for long-range change. The plot of reaction yield of PE tetraester shows that CPKFAs/

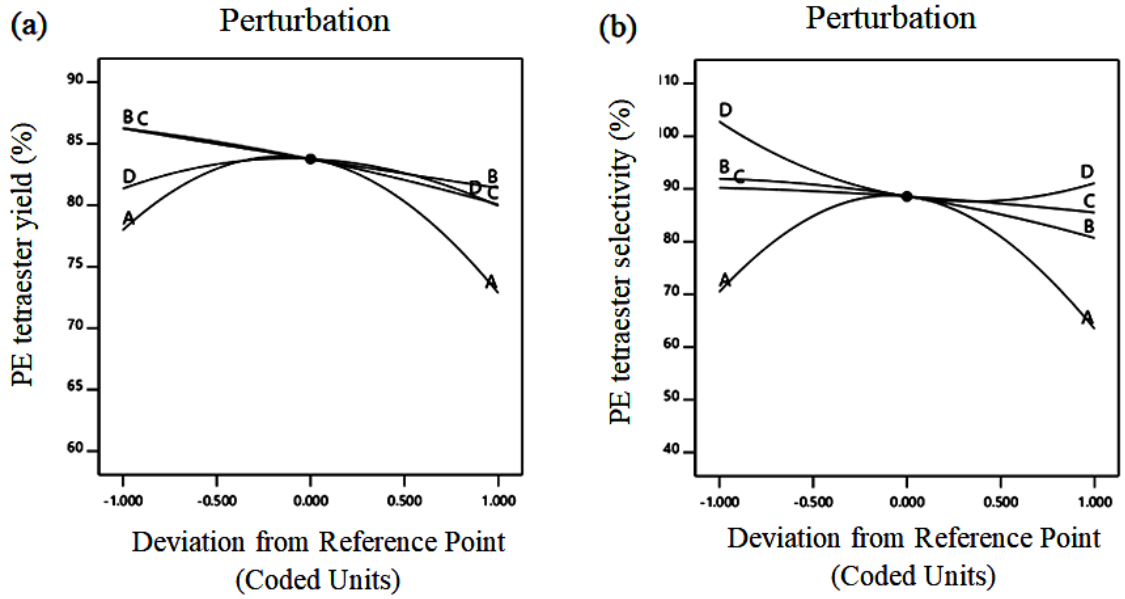

FIGURE 5. Perturbation effect plot of all the factors CPKFAs/PE ratio (A), reaction time (B), reaction temperature (C), and catalyst amount (D) for (a) PE tetraester yield and (b) PE tetraester selectivity by RSM

PE ratio, reaction time, and reaction temperature have a negatively significant effect towards the yield as the level changed from low to high. However, the catalyst amount appears to have a relatively positive effect on the yield from low to medium level and a lower slope compared to CPKFAs/PE ratio, reaction time, and reaction temperature. Apparently, among all four parameters, it is notable that the slope CPKFAs/PE ratio is steeper, thereby virtually indicates that CPKFAs/PE ratio is the most sensitive factor among other parameters. It is noteworthy that the value of the PE tetraester yield increased when CPKFAs/PE ratio, reaction time, and reaction temperature are at a low level as shown in Figure 5(a).

Figure 5(b) shows how CPKFAs/PE ratio (A), reaction time (B), reaction temperature (C), and catalyst amount (D) have on PE tetraester selectivity. A steep curvature of CPKFAs/PE ratio and catalyst amount indicates the high sensitivity towards PE tetraester selectivity, followed by reaction time and temperature. It was understood from this plot that maximum PE tetraester selectivity can be achieved when CPKFAs/PE ratio is at a medium level, whereas the reaction time, and reaction temperature, and catalyst amount at the lowest level.

TABLE 5. The optimum condition for synthesis of TMP triester, di-TMP tetraester, and PE tetraester

Products		Parameters				Responses	
		A	B	C	D	Yield (%)	Selectivity (%)
TMP triester	Predicted	3.05:1	6	150	1.01	87.77	99.15
	Actual average	3.05:1	6	150	1.01	86.13±0.7	99.13±0.4
Di-TMP tetraester	Predicted	4:1	6.0	156	1.0	84.04	93.1
	Actual average	4:1	6.0	156	1.0	83.23±0.5	92.7±0.5
PE tetraester	Predicted	4.16:1	4	168	1.7	87.25	95.7
	Actual average	4.16:1	4	168	1.7	85.9±0.8	95.2±0.5

Notes: A: CPKFAs/ polyhydric alcohols ratio (mol: mol); B: Reaction time (h); C: Reaction temperature (°C); D: Catalyst amount (H_2SO_4) (%)

The estimated factors from the numerical optimization of synthesizing TMP triesters, Di-TMP tetraesters, and PE tetraesters were shown in Table 5. With the case of TMP triesters, the optimum condition forecasted with D-optimal design has generated the ratio of CPKFA/TMP to be 3.05 :1 (mol:mol), with 6 h of reaction time, 150 °C of reaction temperature, and 1.01 % of catalyst to be used (H_2SO_4). Under the given condition, the yield of TMP triesters was quite impressive with 87.77%, and the selectivity was 99.15%. Meanwhile, the forecasted design generated for the synthesis of Di-TMP tetraesters was 4:1 (mol:mol) ratio of CPKFA/Di-TMP reaction time of 6 h, temperature of 156 °C, and 1% of catalyst (H_2SO_4). This condition has generated 84.04% of di-TMP tetraesters yield with 93.10% Di-TMP tetraesters selectivity. For PE tetraesters, the optimum condition forecasted with D-optimal design has generated the ratio of CPKFA/PE to be 4.16:1 (mol:mol), with 4 h of reaction time, 167.7 °C of reaction temperature, and 1.67% of catalyst to be used (H_2SO_4). Under the given condition, the yield of CPKFAs-PETE was quite impressive with 87.25%, and the selectivity was 95.70%. As given in Table 5, three replications of the experiment were done to ensure the accuracy of the predicted model. This produced an average 86.13±0.7% yield and 99.13±0.4% of selectivity in the synthesis of TMP triesters. Additionally, an average 83.23±0.5% of yield and 92.7±0.5% of the selectivity was obtained in the synthesis of Di-TMPt etraesters. Meanwhile, an average 85.9±0.8% of yield and 95.2±0.5% of the selectivity was obtained in the synthesis of PE tetraesters. The confirmation results appeared to be in good agreement with the experimental

results. Therefore, it is emphasized that D-optimal design is a reliable, simple, and useful approach for assessing the best conditions to synthesize TMP triesters, Di-TMP tetraesters, and PE tetraesters.

STRUCTURAL CHARACTERIZATION OF POLYOL ESTERS

Molecular characterization was performed to prove the formation of the ester group in all the esterification products. The presence of the ester group was validated using the FTIR spectroscopy analysis technique. According to Pavia et al. (2015), characteristic peak of stretching vibration of the carbonyl group for aliphatic esters are present in the range of 1735-1810 cm^{-1}, while the C-O esters are denoted by the characteristic peak of stretching vibration of the ester carbonyl group in the range of 1000 to 1300 cm^{-1}. Figure 6 compared the infrared spectra of CPKFAs and products to confirm the presence of related functional groups. Based on Figure 6, the carboxylic acid of CPKFAs peaks (1707 cm^{-1}) has been disappeared and replaced by the ester group's appearance signifying polyol esters' production at a wavenumber of 1743 cm^{-1}. The infrared spectra confirmed that all those lubricant products had been successfully synthesized since the related functional groups of reactants have been converted to the esters group profile and belong to the products. The peak observed at 1741 cm^{-1} of (TMP triesters and Di-TMP tetra ester), and 1740 cm^{-1} of PE tetraesters is characteristic of the stretching vibration of the formation of the ester carbonyl group (-COOR). The bands observed at 1234 and 1152 cm^{-1} in all synthesized polyol esters indicate C-O-C ester linkage, confirming the ester functionalities in all the esterification products.

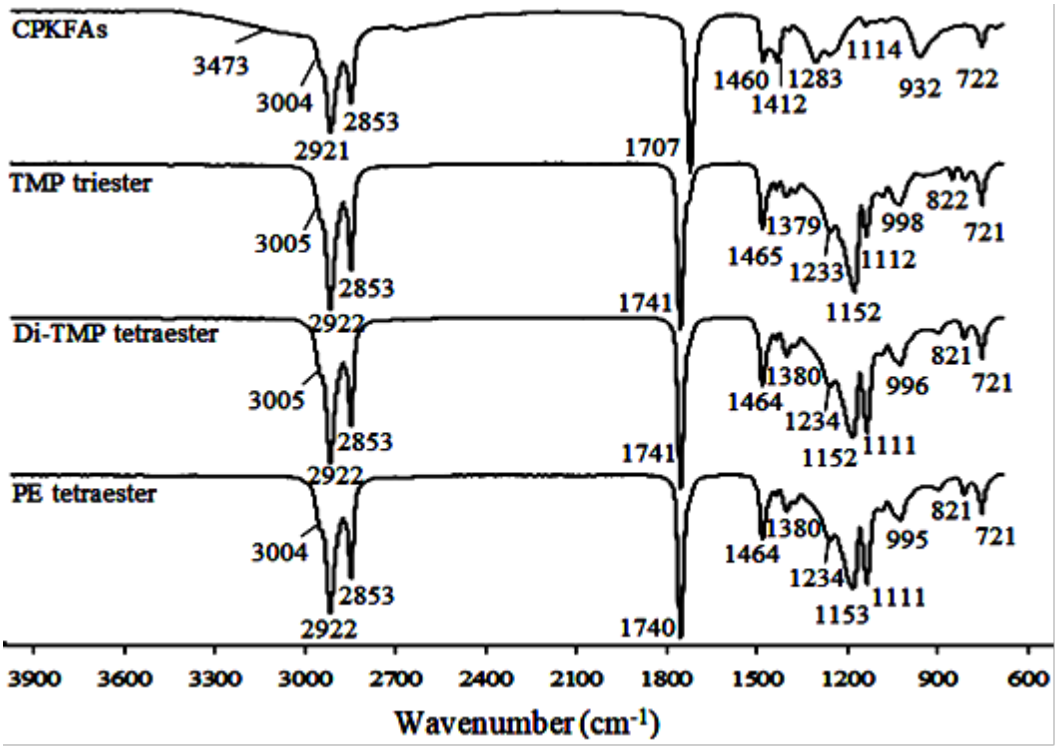

FIGURE 6. FTIR spectrum before and after esterification reaction of TMP triesters

The ^{1}H NMR spectrum displays the effects of the modification performed in the raw material (CPKFAs) by esterification reaction with polyhydric alcohol (TMP, Di-TMP, and PE), as seen in (Figure 7, TMP triesters, di-TMP tetraesters, and PE tetraesters). Two types of hydrogen can verify the ester formation and confirm that the ester has indeed formed. The first belongs to the proton of the carbon atom attached to the oxygen atom in the ester's alcohol part. While the second belongs to the carbon proton in the acid part of the ester. Per Pavia et al. (2015), the current study identified the proton of the alcohol on (-CH_2-O-), i.e., the carbon bonded to the

oxygen atom and (CH_2-C=O), i.e., the proton of the acid part on carbon α. The acid (CH_2C=O) proton was found at the NMR spectrum peak of 2.25-2.29 ppm. In contrast, the alcohol (-CH_2-O-) proton of the CPKFA-based polyol esters was found at 3.96-4.61 ppm. This result is in line with previous works, which found that proton alcohol exhibited a chemical shift at 3.5-4.8 ppm and 2.1-2.5 ppm for proton acid (Pavia et al. 2015).

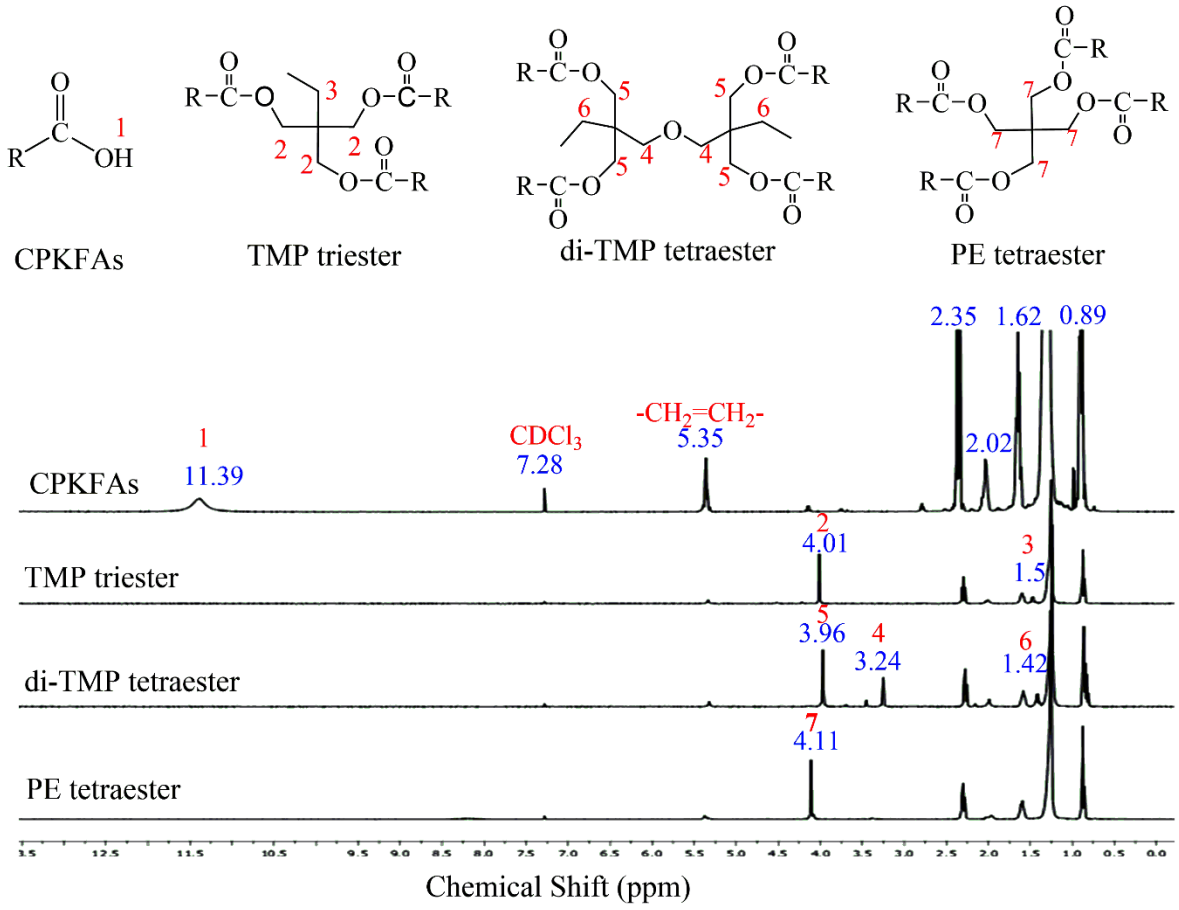

FIGURE 7. The ^{1}H-NMR spectrum of synthesized polyol esters

The ^{13}C NMR spectra of CPKFAs-based polyol esters were established in Figure 8. Signal peaks of 173.49, 173.48, and 173.24 ppm were observed, correlating to the carbon atom in the ester carbonyl (C=O) of TMP triesters, the Di-TMP tetraesters, and the PE tetraesters), respectively. Pavia et al. (2015) also found a chemical shift occurring at 155-185 ppm, attributed to carbon ester carbonyl (C=O). Meanwhile, signal peaks were observed at 63.65, 64.07, and 62.33 ppm attributed to the C-O bonded to the fatty acid (CPKFAs) of the polyhydric alcohols (TMP triesters, di-TMP tetraesters, and PE tetraesters, respectively). The carbon bonds above signal the polyol esters (the ester bond between CPKFAs and the polyhydric alcohols (TMP, Di-TMP, and PE).

POLYOL ESTERS COMPOSITION

The GC-FID analysis showed that the CPKFA-based polyol esters were more than 95% pure. Figure 9(a) to 9(e) shows the results of the GC analysis of the CPKO and CPKFA raw materials before esterification, and TMP triesters, Di-TMP tetraesters, and PE tetraesters after esterification. The results show that three progressive reactions occurred in the intermediate formation of the monoester, diester, and triesters of TMP, based on the three -OH groups in TMP. For Di-TMP and PE, there were four OH groups, signifying four progressive reactions in the intermediate formation of the monoester, diester, trimester, and tetraesters Di-TMP, and PE, respectively. After esterification, the GC peaks of the polyol esters

were compared to triacylglycerol (TAG) as a standard, per Mahmud et al. (2015) and Yunus et al. (2002). The results show that the triacylglycerol (TAG) peaks appeared at 32 to 51 min before hydrolysis, as shown in Figure 9(a). After hydrolysis, the CPKFA peaks occurred at 7 to 15 min, as per Figure 9(b). Triacylglycerol (TAG) CPKO standards were compared to the TMP triesters GC peaks post-esterification, as per Figure 9(a). As shown in the comparison of Figure 9(c) results, the TMP triesters peaks coincided with these peaks at 32-51 min. This result indicates that up to 99% of the triesters was obtained. In Figure 9(d) and 9(e), the peaks of Di-TMP tetraesters and PE tetraesters appeared after 45-67 min in contrast to the triacylglycerol (TAG) standard of CPKO. This was due to increasing its molecular weight, proving the formation of the di-TMP tetraesters and PE tetraesters.

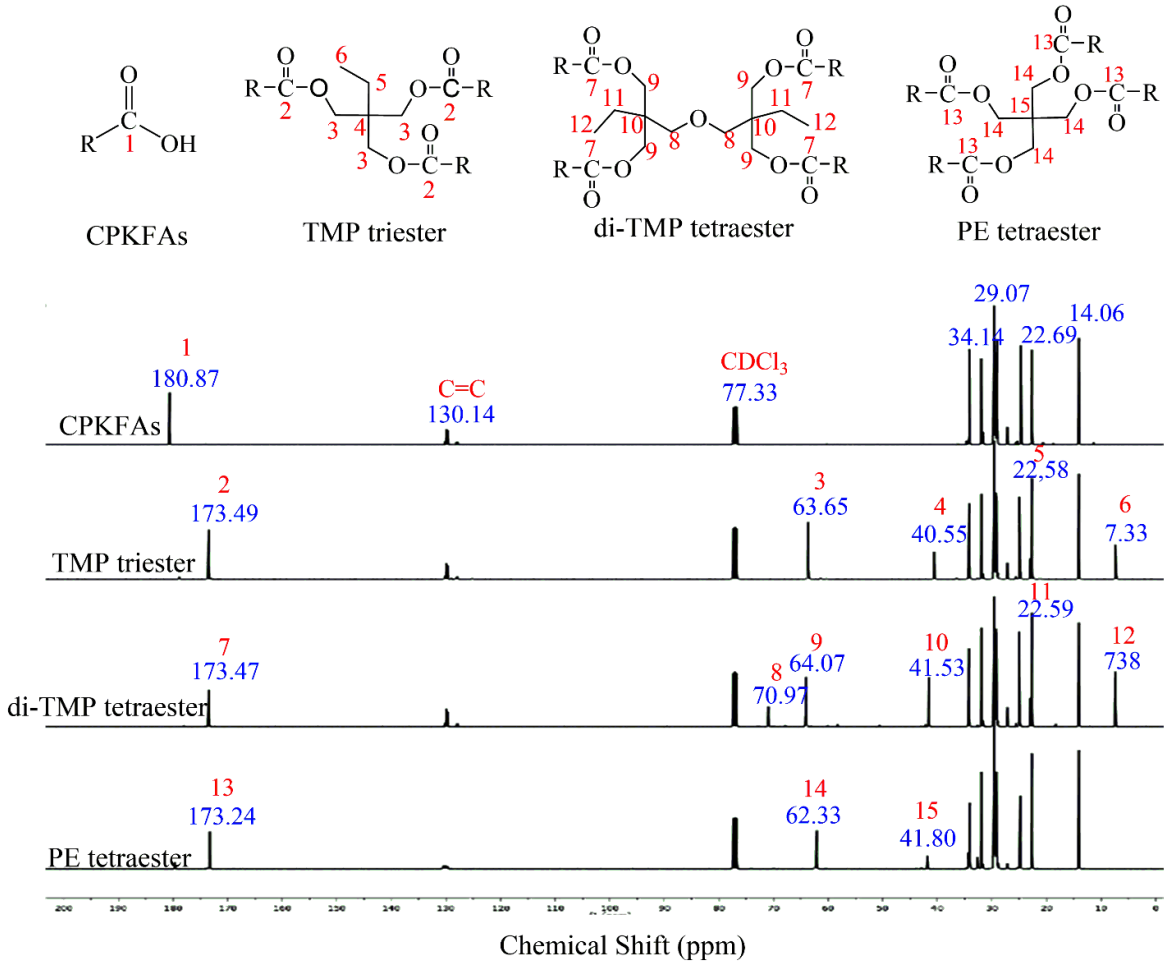

FIGURE 8. The ^{13}C-NMR spectrum of synthesized polyol esters

FATTY ACIDS COMPOSITION

The polyol esters were produced by an average yield of 80-87 wt.%. Figure 10 summarized the fatty acids composition of CPKFAs, TMP triesters, Di-TMP tetraesters, and PE tetraesters. The percentage of saturated fatty acids in TMP triesters, Di-TMP tetraesters, and PE tetraesters were 80.9, 83.1, and 88.1%. The percentage of unsaturated fatty acids of TMP triesters, Di-TMP tetraesters, and PE tetraesters was 19.1, 16.9, and 11.9%, respectively. As shown in Figure 10, the polyol esters derived in this study had similar fatty acid compositions to raw CPKO.

THERMAL STABILITY

Thermal stability of crude palm kernel oil (CPKO), crude palm kernel fatty acids (CPKFAs), and polyol esters-based biolubricant (TMP triester, Di-TMP tetraester, and PE tetraester) was studied by the Thermogravimetric

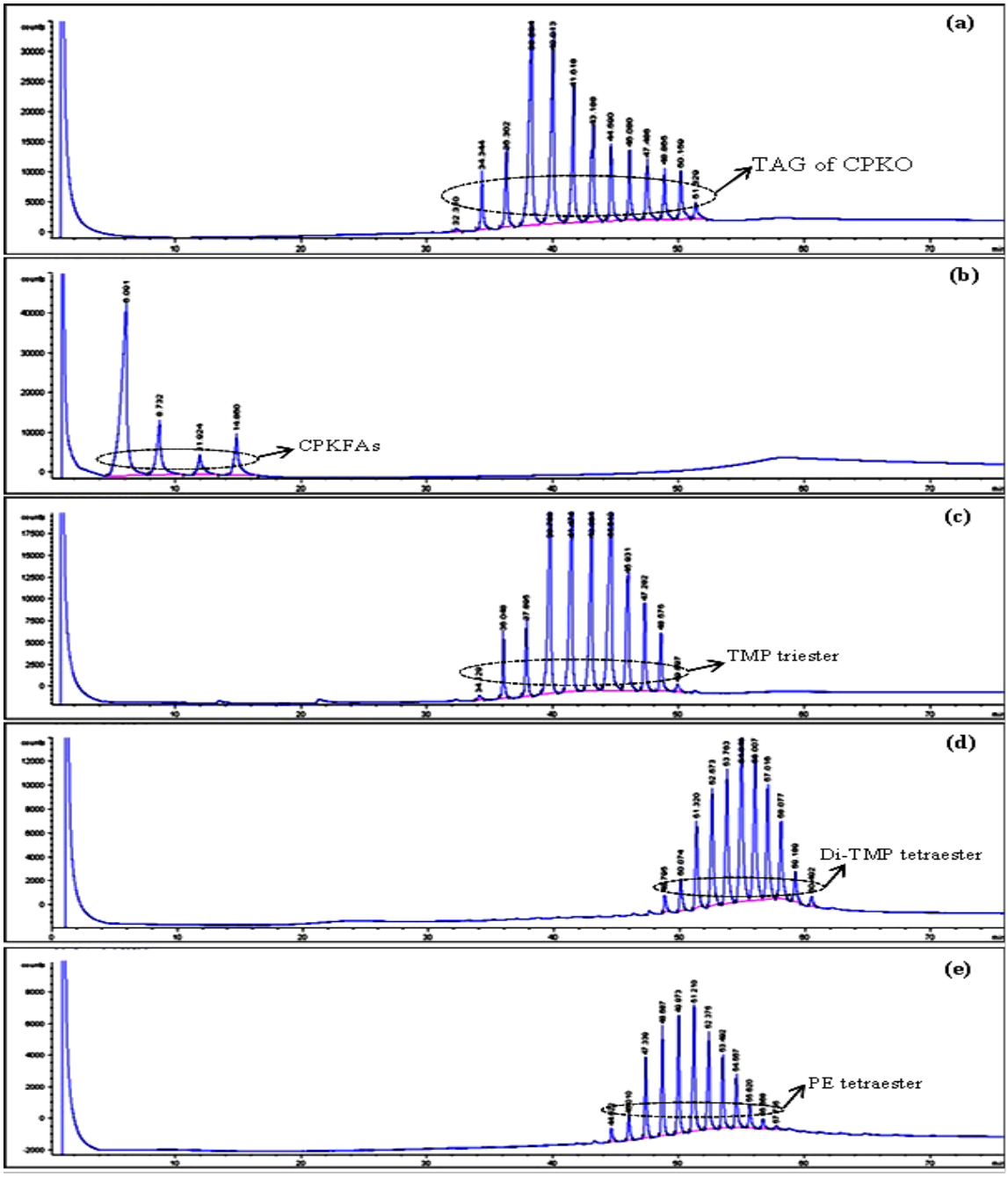

FIGURE 9. Gas chromatogram of (a) CPKO, (b) CPKFAs, (c) TMP triesters, (d) Di-TMP tetraesters, and (e) PE tetraesters

differential thermal analyzer (TGA/DTA). The graphs of weight loss against temperature are shown in Figure 11(A). It is clear from the graph that polyol esters-based biolubricant (TMP triester, Di-TMP tetraester, and PE tetraester) are thermally stable below 372.74, 439.63, and 400.32 °C, respectively. Maximum weight loss (90 wt.%) was observed in all these three polyols esters-based biolubricant (TMP triester, Di-TMP tetraester, and PE tetraester) at temperatures 443.24, 471.88, and 458.47 °C, respectively (Table 6). Hence, it is conclusive that polyol esters-based biolubricant (TMP triester, Di-TMP tetraester, and PE tetraester) are thermally more stable as

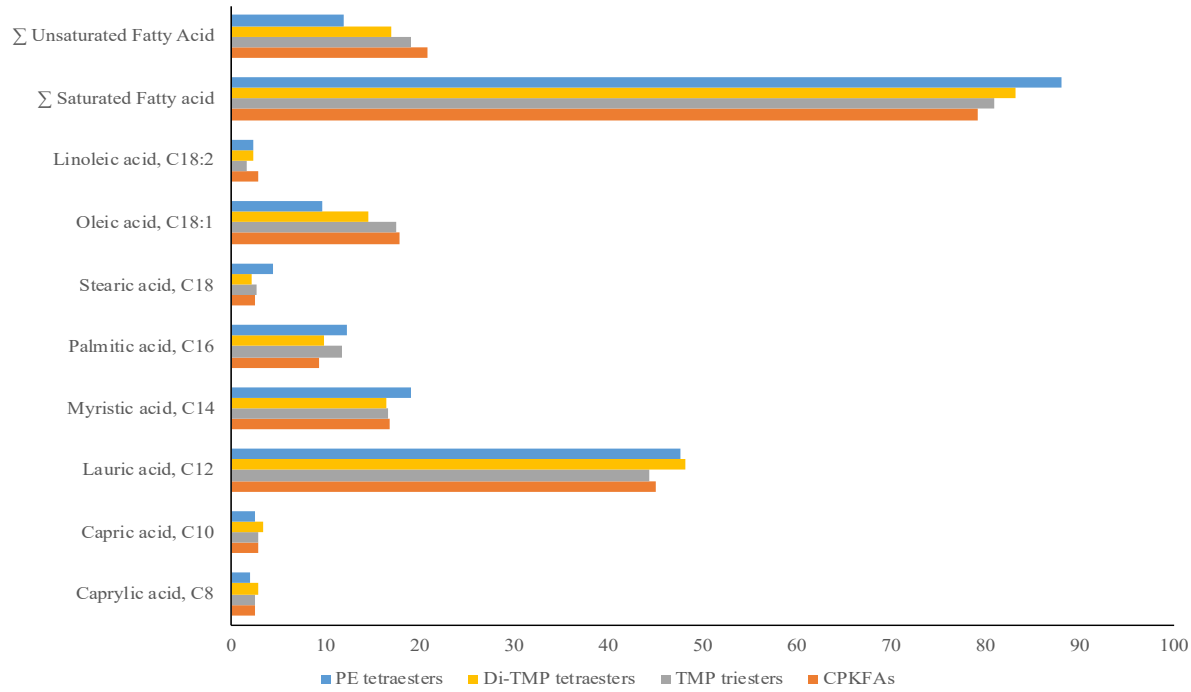

FIGURE 10. Fatty acids composition of CPKFAs, TMP triesters, Di-TMP tetraesters, and PE tetraesters

compared to crude palm kernel oil and crude palm kernel fatty acid which can be due to the absence of β-hydrogen in esters improves the thermal stability of polyol esters-based biolubricant (TMP triester, Di-TMP tetraester, and PE tetraester). Thermogravimetric analysis (TGA) also confirms that the polyol esters-based biolubricant (TMP triester, Di-TMP tetraester, and PE tetraester) can be more useful for high temperature applications. The derivative of the thermogravimetric (DTA) curve showed that the thermodegradation of CPKO, CPKFAs, and its derivatives polyol esters-based biolubricant (TMP triester, Di-TMP tetraester, and PE tetraester) occurs in one thermal peak (Figure 11(B)). For this thermal peak, T_{DTA} for Di-TMP tetraester and PE tetraester around 36 °C higher than TMP triester. Thus, Di-TMP tetraester and PE tetraester were suggested to be more stable, followed by TMP triester.

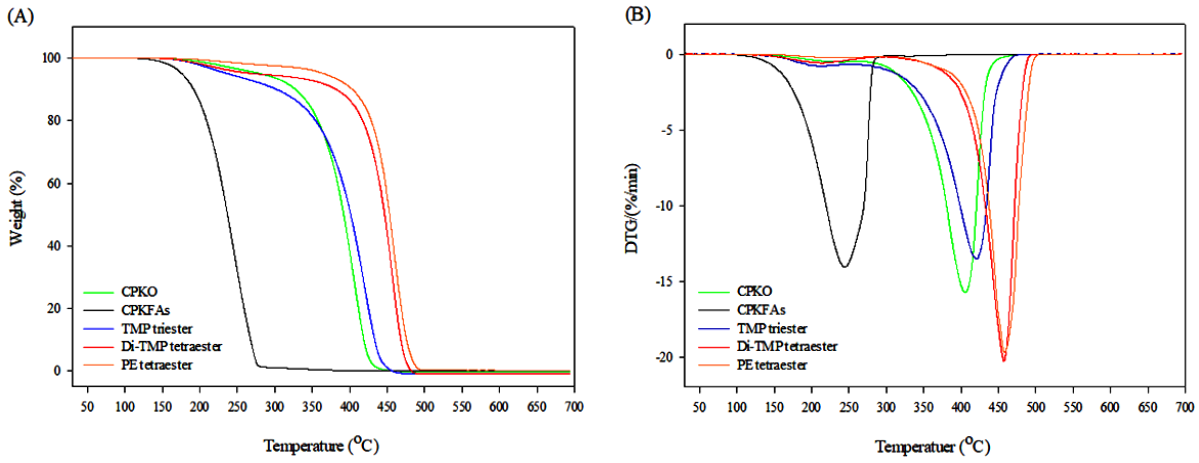

FIGURE 11. (A) TGA curve of CPKO, CPKFAs, TMP triester, Di-TMP tetraester, and PE tetraester. (B) DTG curve of CPKO, CPKFAs, TMP triester, Di-TMP tetraester, and PE tetraester

TABLE 6. Thermal stability and degradation profile of CPKO and the prepared polyol esters-based biolubricant

Product	Temperature (°C)					
	Onset	Endset	10% wt. loss	50% wt. loss	90% wt. loss	DTA(T_{DTA})
CPKO	356.40	426.53	326.61	392.21	419.46	400.89
CPKFAs	189.50	255.52	176.22	220.77	251.52	229.81
TMP triester	372.74	449.40	311.79	411.17	443.24	429.09
Di-TMP tetraester	439.63	472.02	397.59	451.74	471.88	457.6
PE tetraester	400.32	461.02	225.39	432.36	458.47	458.1

PHYSICOCHEMICAL AND LUBRICATION PROPERTIES

The physicochemical properties (acid value and density) and the lubricant properties (thermal stability, flash point, viscosity at 40 and 100 °C, pour point, viscosity index (VI)) of the CPKFA-based polyol esters were characterized and the results presented in Table 7. The changes in viscosity under different temperatures are reflected by kinematic viscosity, which indicates the internal resistance to flow when subjected to gravitational forces. This viscosity temperature property is an important determinant of the performance and application of the lubricant.

The TME triesters, Di-TME tetraesters, and PE tetraesters recorded their kinematic viscosities (40 °C; 100 °C) about 41.76, 86.25, and 87.06 cSt, respectively; and 8.73, 14.77, and 14.55 cSt, respectively. It can be observed that the more acyl functionalities in the polyol esters, the higher their viscosity (Mahmud et al. 2015). All the synthesized CPKFAs-based polyol esters yielded a high viscosity index (more than 140 cSt) and therefore have good potential as lubricants. The higher the viscosity index, the better the lubricant. A high viscosity index indicates that the lubricant's viscosity does not change over a wide range of temperatures and will perform better. A potential lubricant can also be evaluated from its pour point, when the liquid can still be poured. The lubricants should have a low pour point for engines in cold climates. Generally, lower pour points have been observed for polyol esters with more short-chain saturated fatty acids (C_4-C_{12}) and more unsaturated fatty acids (Schneider 2006; Yunus et al. 2004). Also, the pour points of polyol esters prepared with complex structures and branched ester possessed lower pour points are very low (Derawi & Salimon 2013). Furthermore, the pour points of CPKFAs-based polyol esters (TMP triesters, Di-TMP tetraesters, and PE tetraesters) were -10, -5, and -8 °C, respectively. In this study, the CPKFA-based polyol esters had high pour points because palm kernel oil only has a 20% unsaturated fatty acid content, which is considered very low. However, TMP triesters had a lower pour point than Di-TMP tetraesters and PE tetraesters, suggesting that the TMP triesters had the best molecular configuration for disrupting molecular packing all the polyol esters in this study. Lubricants with low pour points are best suited for hydraulic systems and machine tool applications (Fadzel et al. 2019).

The flash point is the lowest temperature at which a liquid can form an ignitable mixture in air near the liquid's surface. According to Keera et al. (2018), high flash point lubricants are desirable because they will not be overly volatile or explode at maximum operating temperature. The potential of fire hazards is greater with low flash point lubricants. The best thermal stability was observed for Di-TMP Tetraesters (flash point at 360 °C), followed by the PE tetraesters and TMP triesters (320 °C flash point). This result is different from those reported for synthetic esters. Esters with a flashpoint of ≥ 165 °C are suitable as hydraulic oils. Per the results above, the CPKFA-based polyol esters had very high flash points ranging from 320 to 360 °C (Tupureina 2009). A lubricant must be thermally stable and should not oxidize or change properties during use (Mortier et al. 2010).

The oxidative point of lubricating oil is a crucial indicator of its quality. When temperatures increase, lubricants could become more corrosive, acidic, viscous, or volatile, so they must resist oxide-forming tendencies as best as possible (Nor et al. 2019). The oxidative stability analysis was performed using Differential Scanning Calorimetry (DSC). Oxidative stability is determined by the temperature onset (TO), which is

when the oxidation rate rapidly increases when the lubricant is subjected to constant high pressure (200 psi). Material has high oxidative stability if it has a high TO (Salimon et al. 2011). In this study, CPKFAs-based polyol esters (TMP triesters, Di-TMP tetraesters, and PE tetraesters) possessed good oxidative stability with high onset temperature 254, 251.8 and 214.62 °C, respectively. It was due to the decreasing percentage of unsaturated fatty acids (20%). The double bond reduction in unsaturated fatty acid had reduced the active oxidation site, which gave higher oxidative stability. All lubricant products are categorized as ISO 46 (TMP triester) and ISO 68 (Di-TMP tetraester and PE tetraester).

TRIBOLOGICAL AND RHEOLOGICAL PROPERTIES

The type of lubricant is usually identified based on the lubricant's tribological properties. Ester has polar groups, making it amphiphilic and enabling it to serve as boundary lubricants. The higher the lubricant polarities, the higher the possibility of reducing wear (Salimon et al. 2012). Oils from plants consist of straight-chain carbon with polar end groups, which give them good lubricity. According to Ahmed et al. (2015), these polar end groups reduce friction coefficient (COF) because they adsorb onto metallic surfaces and decrease surface energy. Figure 12(a) and 12(b) shows the tribological properties of the CPKFA-based polyol esters (TMP triesters, Di-TMP tetraesters, and PE tetraesters). It was noted that the high molecular weight and viscosity of the polyol esters impacted the values of the friction coefficient. The results indicated that the friction coefficient of di-TMP tetraesters was lower than TMP triesters and PE tetraesters at 100 °C because it has a high viscosity and high molecular weight. Generally, despite the low molecular weight of TMP triesters and PE tetraesters, the coefficient of friction of both was still low (with all the polyol esters having a COF below 0.25 at 40 and 100 °C) because these CPKFA-based polyol esters (TMP triesters, Di-TMP tetraesters, and PE tetraesters) had a high polarity. These findings show that the polyol esters maintained good tribological properties even at high temperatures. Since all of the polyol esters had a low coefficient of friction at 40 and 100 °C, they could serve as boundary lubricants.

A rheology analysis was done on the CPKFAs-based polyol esters (TMP triesters, Di-TMP tetraesters, and PE tetraesters) in which shear stress was plotted against shear rate, per Figure 13. This plot helps identify the nature of the fluid, whether Newtonian or non-Newtonian. When a Newtonian fluid's shear rate increases, its viscosity will not change, but the opposite is true for non-Newtonian fluid (Derawi & Salimon 2013). Based on Figure 13, TMP triesters di-TMP tetraesters, and PE tetraesters proved Newtonian fluids.

TABLE 7. Characterization of crude palm kernel fatty acids-based polyol esters

Property	Standard Method	TMP triesters (product[1])	Di-TMP tetraesters (product[2])	PE tetraesters (product[3])
Yield (% wt)	-	86.13	81.65	80.85
Conversion (% GC)	-	99.13	96.71	96.23
Iodine value	AOCS Cd 1-25	17.8	17.7	15.8
FFA %	AOCS Cd 3d-63	2.0	3.2	2.1
Density (25 °C)	ASTM D-4052	0.88	0.88	0.88
Pour point (°C)	ASTM D-97	-10	-5	-8
Flashpoint (°C)	ASTM D-93	320	360	320
Viscosity at 100 °C (cSt)	ASTM D-445	8.73	14.77	14.55
Viscosity at 40 °C (cSt)	ASTM D-445	41.76	86.25	87.06
Viscosity index	ASTM -2270	154.8	142.37	140.86
Oxidative Stability (°C)	ASTM D-6186		251.86	214.62
Friction Coefficient (μ) at 40 °C	ASTM D4172-94	0.17	0.19	0.18
Friction Coefficient (μ) at 100 °C	ASTM D4172-94	0.25	0.17	0.20
Lubricant Grade	ISO 3448	46	68	68

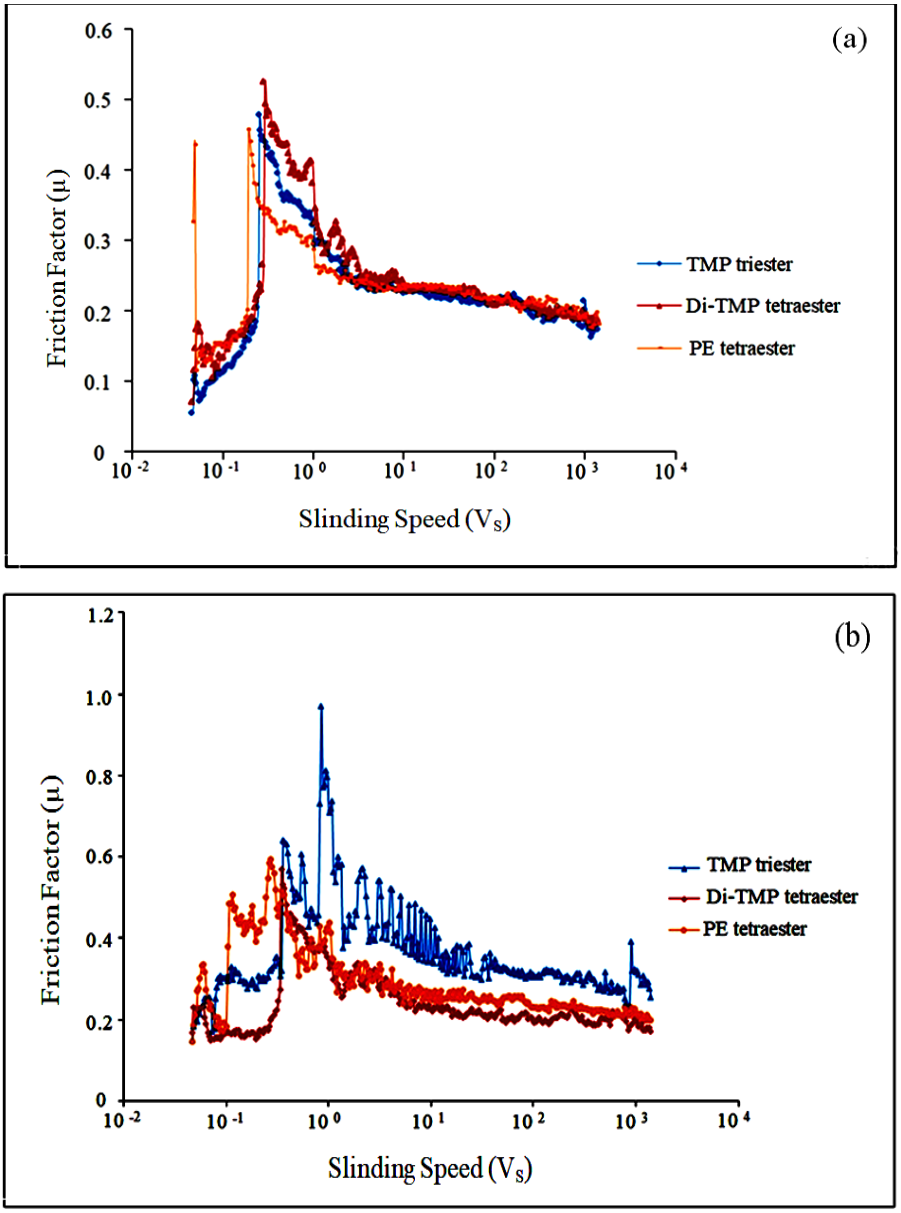

FIGURE 12. The effect of the sliding speed on the friction coefficient at 40 °C (a) and 100 °C (b) of synthesized polyol esters

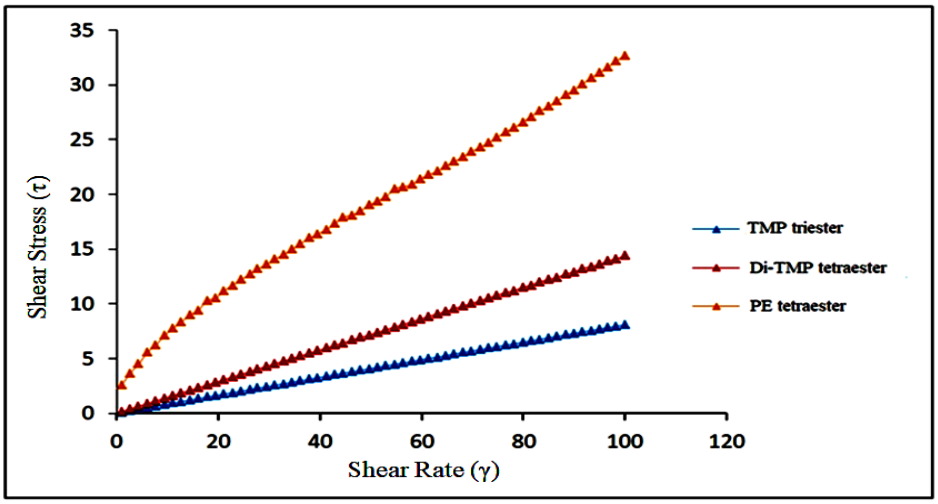

FIGURE 13. Shear stress vs. shear rate plots of synthesized polyol esters at 25 °C

Conclusion

A great demand for renewable lubricant is expected over the next few years compared to the mineral oil-based lubricant. Biolubricant lubricant offers sustainable development, especially water pollution control, and improves environmental quality. Hence, three bio-based lubricant products (TMP triester, Di-TMP tetraester, and PE tetraester) were successfully synthesized and characterized. TMP triester was classified as ISO 46 grade lubricant, while Di-TMP tetraester and PE tetraester were ISO 68 lubricants. All products are considered as a Newtonian fluid. They can be used as hydraulic fluids for machining purposes, either in food or non-food industries based on their lubricant grade.

ACKNOWLEDGEMENTS

The researcher would like to thank Mr. Hasanudin Saleh for the technical support provided. The authors would like to thank the Ministry of Higher Education, Malaysia for the research funding (FRGS/1/2020/STG04/UKM/02/1) and Universiti Kebangsaan Malaysia for providing research facilities and financial support through the research grant no. DIP-2020-007. Condolences are also extended to all COVID-19 victims worldwide, especially in Malaysia.

REFERENCES

Abdullah, B.M., Zubairi, S.I., Huri, H.Z., Hairunisa, N., Yousif, E. & Basu, R.C. 2016. Polyesters based on linoleic acid for biolubricant basestocks: Low-temperature, tribological and rheological properties. *PLoS ONE* 11(3): e0151603.

Agrawal, A.J., Karadbhajne, V.Y., Agrawal, P.S., Arekar, P.S. & Chakole, N.P. 2017. Synthesis of biolubricants from non edible oils. *International Research Journal of Engineering and Technology* 4(7): 1753-1757.

Ahmed, W.A., Yarmo, A., Salih, N., Derawi, M.D. & Yusop, M.R. 2015. Synthesis and lubricity properties analysis of branched dicarboxylate esters based lubricant. *Malaysian Journal of Analytical Sciences* 19(1): 106-117.

Aigbodion, A.I. & Bakare, I.O. 2005. Rubber seed oil quality assessment and authentication. *Journal of the American Oil Chemists' Society* 82(7): 465-469.

Alam, A.S.A.F., Er, A.C. & Begum, H. 2015. Malaysian oil palm industry: Prospect and problem. *Journal of Food, Agriculture and Environment* 13(2): 143-148.

Algoufi, Y.T., Kabir, G. & Hameed, B.H. 2017. Synthesis of glycerol carbonate from biodiesel by-product glycerol over calcined dolomite. *Journal of the Taiwan Institute of Chemical Engineers* 70: 179-187.

Awang, R., Ghazuli, M.R. & Basri, M. 2007. Immobilization of lipase from *Candida rugosa* on palm-based polyurethane foam as a support material. *American Journal of Biochemistry and Biotechnology* 3(3): 163-166.

Aziza, N.A., Yunus, R., Rashida, U. & Syama, A. 2014. Application of response surface methodology (RSM) for optimizingthe palm-based pentaerythritol ester synthesis. *Industrial Crops and Products Journal* 62: 305-312.

Ba-Abbad, M.M., Kadhum, A.A.H., Mohamad, A.B., Takriff, M.S. & Sopian, K. 2013. Optimization of process parameters using D-optimal design for synthesis of ZnO nanoparticles via sol-gel technique. *Journal of Industrial and Engineering Chemistry* 19(1): 99-105.

Bahadi, M., Salimon, J. & Derawi, D. 2021. Synthesis of di-trimethylolpropane tetraester-based biolubricant from *Elaeis guineensis* kernel oil via homogeneous acid-catalyzed transesterification. *Renewable Energy* 171: 981-993.

Bahadi, M., Yusoff, M.F., Salimon, J. & Derawi, D. 2020. Optimization of response surface methodology by d-optimal design for alkaline hydrolysis of crude palm kernel oil. *Sains Malaysiana* 49(1): 29-41.

Bahadi, M.A., Japir, A.W., Salih, N. & Salimon, J. 2016. Free fatty acids separation from Malaysian high free fatty acid crude palm oil using molecular distillation. *Malaysian Journal of Analytical Sciences* 20(5): 1042-1015.

Bart, J.C.J., Gucciardi, E. & Cavallaro, S. 2012. *Biolubricants: Science and Technology.* Oxford: Woodhead Publishing Limited.

Bhan, C., Verma, L. & Singh, J. 2020. Alternative fuels for sustainable development. In *Environmental Concerns and Sustainable Development*, edited by Shukla, V. & Kumar, N. Singapore: Springer. pp. 317-331.

Bölük, G. & Mert, M. 2014. Fossil & renewable energy consumption, GHGs (greenhouse gases) and economic growth: Evidence from a panel of EU (European Union) countries. *Energy* 74(C): 439-446.

Cavalcanti, E.D.C., Aguieiras, É.C.G., da Silva, P.R., Duarte, J.G., Cipolatti, E.P., Fernandez-Lafuente, R., da Silva, J.A.C. & Freire, D.M.G. 2018. Improved production of biolubricants from soybean oil and different polyols via esterification reaction catalyzed by immobilized lipase from *Candida rugosa*. *Fuel* 215: 705-713.

Derawi, D. & Salimon, J. 2013. Palm olein based biolubricant basestocks: Synthesis, characterisation, tribological and rheological analysis. *Malaysian Journal of Analytical Sciences* 17(1): 153-163.

Dujjanutat, P. & Kaewkannetra, P. 2020. Production of bio-hydrogenated kerosene by catalytic hydrocracking from refined bleached deodorised palm/palm kernel oils. *Renewable Energy* 147: 464-472.

Fadzel, F.M., Salimon, J. & Derawi, D. 2019. Biolubricant production from palm stearin fatty acids and pentaerythritol. *Malaysian Journal of Chemistry* 21(2): 50-63.

Goon, D.E., Abdul Kadir, S.H.S., Latip, N.A., Rahim, S.A. & Mazlan, M. 2019. Palm oil in lipid-based formulations and drug delivery systems. *Biomolecules* 9(2): 1-20.

Gupta, V.G., Tuohy, M., Kubicek, C.P., Saddler, J. & Xu, F. 2013. *Bioenergy Research: Advances and Applications*. Amsterdam: Newnes. pp. 1-500.

Japir, Salimon, J., Derawi, D., Bahadi, M., Al-Shuja'A, S. & Yusop, M.R. 2017. Physicochemical characteristics of high free fatty acid crude palm oil. *OCL - Oilseeds and fats, Crops and Lipids* 24(5): D506.

Japir, A.A.W., Salimon, J., Derawi, D., Bahadi, M. & Yusop, M.R. 2016. Purification of high free fatty acid crude palm oil using molecular distillation. *Asian Journal of Chemistry* 28(11): 2549-2554.

Karmakar, A., Karmakar, S. & Mukherjee, S. 2010. Properties of various plants and animals feedstocks for biodiesel production. *Bioresource Technology* 101(19): 7201-7210.

Keera, S.T., El Sabagh, S.M. & Taman, A.R. 2018. Castor oil biodiesel production and optimization. *Egyptian Journal of Petroleum* 27(4): 979-984.

Kushairi, A., Ong-Abdullah, M., Nambiappan, B., Hishamuddin, E., Bidin, M.N.I.Z., Ghazali, R., Subramaniam, V., Sundram, S. & Parveez, G.K.A. 2020. Oil palm economic performance in Malaysia and R&D progress in 2019. *Journal of Oil Palm Research* 31(2): 159-190.

Mahmud, H.A., Salih, N. & Salimon, J. 2015. Oleic acid based polyesters of trimethylolpropane and pentaerythritol for biolubricant application. *Malaysian Journal of Analytical Sciences* 19(1): 97-105.

Mang, T. & Dresel, W. 2017. *Lubricants and Lubrication.* Weinheim, Germany: Wiley-VCH. pp. 1-890.

Mintova, S. & Ng, E. 2015. Zeolite nanoparticles as effective antioxidant additive for the preservation of palm oil-based lubricant. *Journal of the Taiwan Institute of Chemical Engineers* 58: 565-571.

Mortier, R.M., Fox, M.F. & Orszulik, S.T. 2010. *Chemistry and Technology of Lubricants.* Dordrecht: Springer Netherlands. pp. 1-457.

Nor, N.M., Derawi, D. & Salimon, J. 2019. Esterification and evaluation of palm oil as biolubricant base stock. *Malaysian Journal of Chemistry* 21(2): 28-35.

Nowicki, J., Stańczyk, D., Drabik, J., Mosio-Mosiewski, J., Woszczyński, P. & Warzała, M. 2016. Synthesis of fatty acid esters of selected higher polyols over homogeneous metallic catalysts. *Journal of the American Oil Chemists' Society* 93(7): 973-981.

Onoja, E., Chandren, S., Abdul Razak, F.I., Mahat, N.A. & Wahab, R.A. 2019. Oil palm (*Elaeis guineensis*) biomass in Malaysia: The present and future prospects. *Waste and Biomass Valorization* 10(8): 2099-2117.

Owuna, F.J., Dabai, M.U., Sokoto, M.A., Dangoggo, S.M., Bagudo, B.U., Birnin-Yauri, U.A., Hassan, L.G., Sada, I., Abubakar, A.L. & Jibrin, M.S. 2019. Chemical modification of vegetable oils for the production of biolubricants using trimethylolpropane: A review. *Egyptian Journal of Petroleum* 29(1): 75-82.

Papadaki, A., Fernandes, K.V., Chatzifragkou, A., Aguieiras, E.C.G., da Silva, J.A.C., Fernandez-Lafuente, R., Papanikolaou, S., Koutinas, A. & Freire, D.M.G. 2018. Bioprocess development for biolubricant production using microbial oil derived via fermentation from confectionery industry wastes. *Bioresource Technology* 267: 311-318.

Pavia, D.L., Lampman, G.M., Kriz, G.S. & Vyvyan, J.R. 2015. *Introduction to Spectroscopy.* Australia: Cengage Learning, Inc. pp. 1-786.

Prasad, S., Kumar, S., Sheetal, K.R. & Venkatramanan, V. 2020. Global climate change and biofuels policy: Indian perspectives. In *Global Climate Change and Environmental Policy*, edited by Venkatramanan, V., Shah, S. & Prasad, R. Singapore: Springer Singapore. pp. 207-226.

Radovanović, M., Filipović, S. & Pavlović, D. 2017. Energy security measurement - A sustainable approach. *Renewable and Sustainable Energy Reviews* 68: 1020-1032.

Resul, M.F.M.G., Tinia, T.I. & Idris, A. 2012. Kinetic study of jatropha biolubricant from transesterification of *Jatropha curcas* oil with trimethylolpropane: Effects of temperature. *Industrial Crops and Products* 38(1): 87-92.

Rios, Í.C., Cordeiro, J.P., Arruda, T.B.M.G., Rodrigues, F.E.A., Uchoa, A.F.J., Luna, F.M.T., Cavalcante, C.L. & Ricardo, N.M.P.S. 2019. Chemical modification of castor oil fatty acids (*Ricinus communis*) for biolubricant applications: An alternative for Brazil's green market. *Industrial Crops and Products* 145: 112000.

Rohman, A., Che Man, Y.B., Ismail, A. & Hashim, P. 2010. Application of FTIR spectroscopy for the determination of virgin coconut oil in binary mixtures with olive oil and palm oil. *Journal of the American Oil Chemists' Society* 87(6): 601-606.

Rudnick, L.R. 2020. *Synthetics, Mineral Oils, and Bio-Based Lubricants Chemistry and Technology*. Boca Raton: CRC Press. pp. 1-1194.

Salih, N., Salimon, J. & Yousif, E. 2013a. The effect of chemical structure on pour point, oxidative stability and tribological properties of oleic acid triester derivatives. *Malaysian Journal of Analytical Sciences* 17(1): 119-128.

Salih, N., Salimon, J., Yousif, E. & Abdullah, B.M. 2013b. Biolubricant basestocks from chemically modified plant oils: Ricinoleic acid based-tetraesters. *Chemistry Central Journal* 7(1): 1-13.

Salih, N., Salimon, J. & Yousif, E. 2011. The physicochemical and tribological properties of oleic acid based triester biolubricants. *Industrial Crops and Products* 34(1): 1089-1096.

Salimon, J., Salih, N. & Yousif, E. 2012. Improvement of pour point and oxidative stability of synthetic ester basestocks for biolubricant applications. *Arabian Journal of Chemistry* 5(2): 193-200.

Salimon, J., Salih, N. & Yousif, E. 2011. Chemically modified biolubricant basestocks from epoxidized oleic acid: Improved low temperature properties and oxidative stability. *Journal of Saudi Chemical Society* 15(3): 195-201.

Schneider, M.P. 2006. Plant-oil-based lubricants and hydraulic fluids. *Journal of the Science of Food and Algriculture* 86: 1769-1780.

Tupureina, V. 2009. Compositions of hydraulic fluids based on rapeseed oil and its derivatives. *Engineering for Rural Development* 28: 171-175.

Wang, E., Ma, X., Tang, S., Yan, R., Wang, Y., Riley, W.W. & Reaney, M.J.T. 2014. Synthesis and oxidative stability of trimethylolpropane fatty acid triester as a biolubricant base oil from waste cooking oil. *Biomass and Bioenergy* 66: 371-378.

Wu, S.Q., Sun, T.T., Cai, Z.Z., Shen, J., Yang, W.Z., Zhao, Z.M. & Yang, D.P. 2020. Biolubricant base stock with improved low temperature performance: Ester complex production using housefly (*Musca domestica* L.) larval lipid. *Renewable Energy* 162: 1940-1951.

Yaseen, M., Abbas, F., Shakoor, M.B., Farooque, A.A. & Rizwan, M. 2020. Biomass for renewable energy production in Pakistan: Current state and prospects. *Arabian Journal of Geosciences* 13(2): 1-13.

Yunus, R., Fakhru'l-Razi, A., Ooi, T.L., Iyuke, S.E. & Perez, J.M. 2004. Lubrication properties of trimethylolpropane esters based on palm oil and palm kernel oils. *European Journal of Lipid Science and Technology* 106(1): 52-60.

Yunus, R., Fakhru'l-Razi, A., Ooi, T.L., Omar, R. & Idris, A. 2005. Synthesis of palm oil based trimethylolpropane esters with improved pour points. *Industrial & Engineering Chemistry Research* 44(22): 8178-8183.

Yunus, R., Lye, O.T., Fakhru'l-Razi, A. & Basri, S. 2002. A simple capillary column GC method for analysis of palm oil-based polyol esters. *Journal of the American Oil Chemists' Society* 79(11): 1075-1080.

Zulkifli, N.W.M., Masjuki, H.H., Kalam, M.A., Yunus, R. & Azman, S.S.N. 2014. Lubricity of bio-based lubricant derived from chemically modified jatropha methyl ester. *Jurnal Tribologi* 1: 18-39.

*Corresponding author; email: darfizzi@ukm.edu.my